MOPSA48

SIMULATION OF THE ELECTROSTATIC DEFLECTOR OF DC140 CYCLOTRON

A.Zabanov†, K. Gikal, G.Gulbekyan, I.Kalagin, N.Kazarinov, V.Lisov, S.Mitrofanov, V.Semin

JINR, Dubna, Moscow region, 141980, Russia

† zabanov@jinr.ru

INTRODUCTION

Flerov Laboratory of Nuclear Reaction of Joint Institute for Nuclear Research carries out the works under the creating of Irradiation Facility based on the DC140 cyclotron [1]. The DC140 will be a reconstruction of the DC72 cyclotron [2, 3].

The extraction system based on four main elements - electrostatic deflector (ESD), focusing magnetic channel, Permanent Magnet Quadrupole lens and steering magnet.

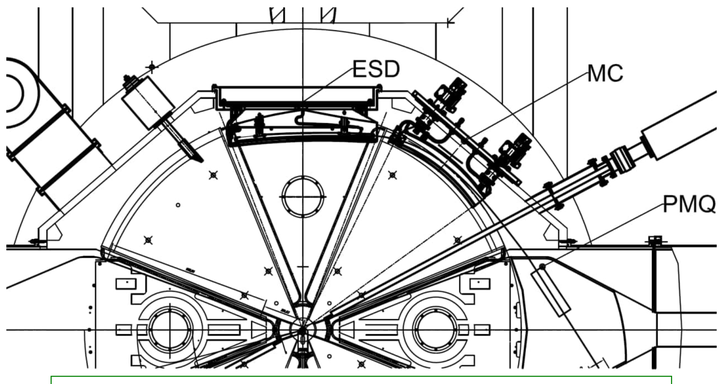

Figure 1: Drawing of extraction system of DC140 cyclotron

The ion beam extraction process from the DC140 cyclotron is implemented using an ESD. The azimuthal extension of ESD is 40º (70º - 110º). Due to the low power of the accelerated ion beams, it was decided that the potential electrode will not have an active cooling system.

This report presents the simulation and comparative analysis of various modifications of an ESD: with a constant and a variable gap.

THE DETERMINATION OF CURVATURE RADIUS OF THE SEPTUM

The extraction orbits of ion beams $^{40}Ar^{8+}$, $^{209}Bi^{38+}$ (W = 4.8 MeV/u), $^{197}Au^{26+}$, $^{132}Xe^{16+}$ (W = 2.124 MeV/u) were used to determine the curvature radius of the septum. The listed ion beam correspond to the corners of the working diagram of DC140 cyclotron.

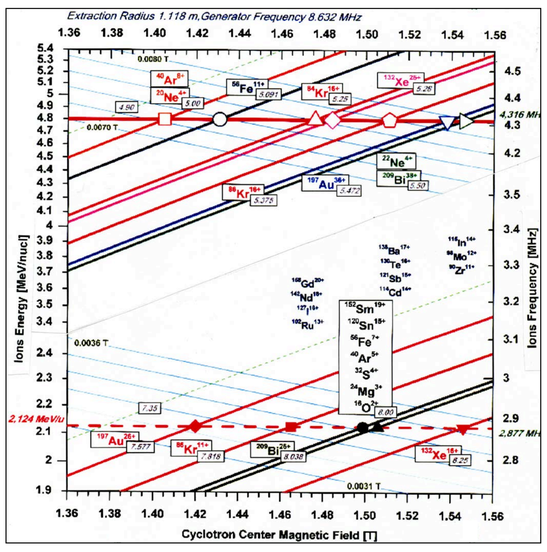

Figure2:Working diagram of DC140 cyclotron

The extraction orbit of ion beam in ESD can be represented as circular arc with center coordinates (x_s; y_s). The optimization task is to find the curvature radius R_s of septum and coordinates of the center (x_s; y_s), which ensure the minimum value of the functional.

$$\frac{1}{n}\sum_{i=1}^{n}(R_s - R_i)^2 \longrightarrow 0$$

where $R_i = \sqrt{(r_i \cdot \cos(\varphi_i) - x_s)^2 + (r_i \cdot \sin(\varphi_i) - y_s)^2}$ is distance from the center coordinates (x_s; y_s) to the i point of the extraction orbit of the ion beam, (r_i , φ_i) are the coordinates of point i of the extraction orbit of the ion beam in cylindrical coordinate system with origin in the cyclotron center.

Table 1: The Optimization Results of the Determination of Curvature Radius of the Septum

Ion	W, MeV/u	$B\rho$, T×m	x_s, cm	y_s, cm	R_s, cm
$^{40}Ar^{8+}$	4.8	1.58	20.87	-200.26	309.28
$^{209}Bi^{38+}$	4.8	1.74	19.01	-176.31	285.68
$^{197}Au^{26+}$	2.124	1.59	20.6	-198.67	307.68
$^{132}Xe^{16+}$	2.124	1.73	19.16	-177.33	286.71

The optimal values of curvature radii of the septum for the ion beams are very different from each other. It is necessary to find the value of the curvature radius, which ensures the minimum beam losses. The curvature radius of the septum was chosen R_s = 301.9 cm. This value was chosen from geometric and design considerations.

THE OPTIMIZATION CURVATURE RADIUS OF THE POTENTIAL ELECTRODE

Two modifications of ESD with a variable gap were considered in the work: with a linearly increasing gap and a linearly decreasing electrostatic field. The ratio of the entrance gap to the exit gap g_1/g_n was varied: 5/8 and 6/9 (mm/mm).

For convenience the following consideration will be performed in the local coordinate system $x'y'$. The center of the origin of coordinates of the local system coincides with the center of curvature of the septum. The ordinate axis y' passes through the center of the septum. The azimuthal extension of ESD $\Delta\varphi'$ in the local system is 14.73º ([90º - $\Delta\varphi'$/2; 90º - $\Delta\varphi'$/2]).

Let us consider in detail the modification of the deflector with a linearly decreasing field. The field potential $F(r', \varphi')$ which provides a linearly decreasing field, is described by:

$$F(r',\varphi') = \frac{U}{\ln(\frac{R'_1}{R_s})} \cdot \ln(\frac{r'}{R_s})$$

where U is potential electrode voltage, R'_1 is distance from the center of coordinates to the inner surface of the potential electrode. The distance R'_1 can be represented by a function of φ'.

$$R'_1(\varphi') = R_s + g(\varphi')$$

The value of the gap $g(\varphi')$ is determined by

$$g(\varphi') = R_s \cdot \exp\left(\frac{1}{C_1 + C_2 \cdot (\varphi' - \varphi'_n)}\right)$$

$$C_1 = \ln\left(\frac{g_n}{R_s} + 1\right)$$

$$C_2 = \left[\frac{1}{\ln\left(\frac{g_1}{R_s}+1\right)} - \frac{1}{\ln\left(\frac{g_n}{R_s}+1\right)}\right] \cdot \frac{1}{\Delta\varphi'}$$

The optimization task is to find curvature radius of the potential electrode R_{pot} and coordinates of the center (x'_{pot}; y'_{pot}), which ensure the minimum value of the functional

$$\frac{1}{n}\sum_{i=1}^{n}(R_{pot} - R'_{1i})^2 \longrightarrow 0$$

Table 2: The Results of Optimization of Radius Curvature of the Potential Electrode

g_1/g_n	x'_{pot}, mm	y'_{pot}, mm	R_{pot}, cm
5/8	11.59	-42.16	306.73
6/9	11.64	-36.54	306.28

THE FIELD OF ESD WITH VARIABLE GAP

The electric field strength $E_{r'}$ and $E_{\varphi'}$ between the electrodes of ESD is described by the following system of equations

$$\begin{cases} E_{r'} = -U \cdot (C_1 + C_2 \cdot (\varphi' - \varphi'_n)) \cdot \dfrac{1}{r'} \\ E_{\varphi'} = -\dfrac{U \cdot C_2 \cdot \ln\left(\dfrac{r'}{R_s}\right)}{r'} \end{cases}$$

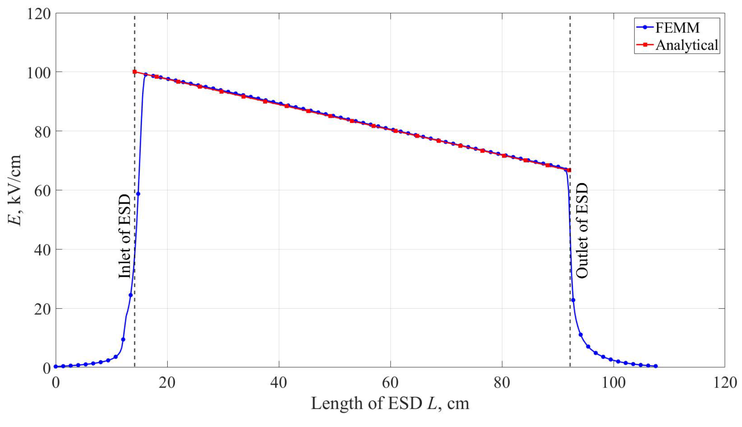

Figure 3: The amplitude value of the electric field strength along the central trajectory of ESD

THE COMPARISON OF VARIOUS MODIFICATIONS OF ESD

This section provides a comparative analysis of three modifications of the ESD: with constant gap g = 9 mm, with a linearly increasing gap and with a linearly decreasing electrostatic field.

All of above modifications of the ESD deflect the ion beam at a given angle, i.e. integral of the electric field strength along the central trajectory of ESD is the same for three modifications.

The beam losses is a key comparison criterion. The total beam losses η on the septum surface is the sum of three components:

- losses at the inlet end face of the septum η_{end}

$$\eta_{end} = \frac{d_s}{\Delta} \cdot 100\%$$

- losses on the inner surface of the septum η_{in}

$$\eta_{in} = \begin{cases} \dfrac{\min(\Delta R_s)^2}{4 \cdot \theta_{max} \cdot \Delta \cdot (L_s - L_{loss})} \cdot 100\%, & \dfrac{|\min(\Delta R_s)|}{L_s - L_{loss}} \le 2 \cdot \theta_{max} \\ \dfrac{\min(\Delta R_s)^2}{4 \cdot \theta_{max} \cdot \Delta \cdot (L_s - L_{loss})} \cdot 100\%, & \dfrac{|\min(\Delta R_s)|}{L_s - L_{loss}} > 2 \cdot \theta_{max} \end{cases}$$

- losses on the outer surface of the septum η_{out}

$$\eta_{out} = \frac{\min(\Delta R)^2}{4 \cdot l_{min} \cdot \theta_{max} \cdot \Delta} \cdot 100\%$$

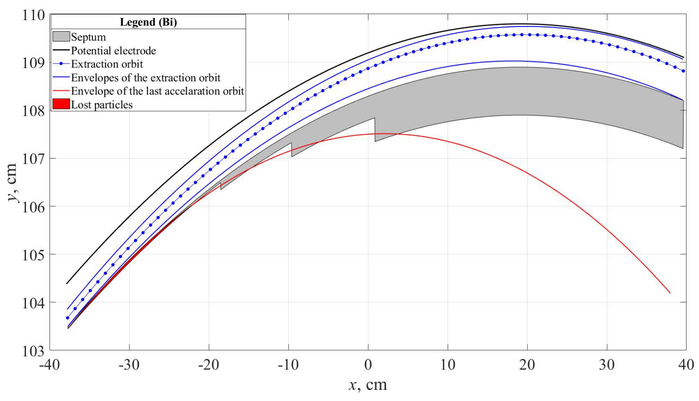

Figure 4:The estimated location of the ESD with constant gap for ion beam $^{209}Bi^{38+}$

Table 3: The Comparison of Various Modifications of ESD

Parameter		Constant gap	Linearly gap 5/8	Linearly gap 6/9	Linearly field 5/8	Linearly field 6/9
U, kV		74	53.44	61.67	50.98	60.02
E_{max}, kV/cm		82.22	103.77	101.44	101.94	99.11
$E_{max} \times U$, kV²/cm		6084.3	5545.5	6255.8	5196.9	5948.6
η_{end}, %	$^{197}Au^{26+}$	10.01	10.88 (0.87)	10.01	10.88 (0.87)	10.01
	$^{209}Bi^{38+}$	13.93	13.93	13.93	13.93	13.93
η_{in}, %	$^{197}Au^{26+}$	1.67	6.41	1.67	6.42	1.92
	$^{209}Bi^{38+}$	0	32.76	9.04	42.97	15.75
η_{out}, %	$^{197}Au^{26+}$	0.09	0.02	0.09	0.02	0.08
	$^{209}Bi^{38+}$	7.32	3.74	6.13	2.84	5.28
η, %	$^{197}Au^{26+}$	11.77	16.45	11.77	17.32	12.02
	$^{209}Bi^{38+}$	21.25	50.44	29.1	59.74	34.96

High precision manufacturing of the potential electrode and its installation relative to the septum are important conditions for ensuring the desired change in the variable gap along the length of the deflector.

The ESD with constant gap between electrodes provides the lowest beam losses at the septum compared to the other modifications.

A big value of the beam losses of ion beam $^{209}Bi^{38+}$ is explained by difference between the selected septum radius of curvature R_s = 301.9 cm and obtained as result of optimization for the extraction orbit (R_{Bi} = 285.68 cm).

REFERENCES

[1] S.V. Mitrofanov et.al., "FLNR JINR Accelerator Complex for Applied Physics Researches: State-of-Art and Future", In Proc. of 22nd Conf. on Cycl. and their Appl., Cape Town, South Africa, Sep. 2019, pp. 358-360, doi:10.18429/JACoW-CYCLOTRONS2019-FRB02

[2] B. N. Gikal, "Dubna Cyclotrons – Status and Plans", in Proc. 17th Int. Conf. on Cyclotrons and Their Applications (Cyclotrons'04), Tokyo, Japan, Oct. 2004, paper 20A1, pp. 100-104.

[3] G. Gulbekyan, I. Ivanenko, J. Franko, and J. Keniz, "DC-72 Cyclotron Magnetic Field Formation", In Proc. of 19th Russian Part. Acc. Conf (RuPAC'04), Dubna, Russia, Oct. 2004, paper WENO12, pp. 147-49.